cues such as the mother's fur. The authors demonstrate that pups that suckle mothers with odorants painted on the doe's belly subsequently perform search and grasp to the conditioned stimulus alone. Is 2MB2 as effective as nursing in promoting the learned association with the conditioned stimulus? This is difficult to answer because the authors employed concentrations of the conditioned stimuli at which the proportion of responding pups reaches saturation (~90%). It should be feasible to resolve this issue in future studies. In any event, these data provide strong evidence that the rabbit suckling pheromone can promote associative learning.

The present study demonstrates that suckling, an innate behavior, can be conditioned by a single pheromone. Previous work has demonstrated that, in many mammals, chemosensory neurons in the nose are segregated into the main olfactory epithelium and the vomeronasal organ. Activation of main olfactory epithelium neurons by odors is thought to elicit measured behavioral output, whereas the vomeronasal organ is thought to recognize pheromones which trigger innate, stereotypical responses [12]. Recent findings, however, suggest that this model is an oversimplification. For example, a putative pheromone in male mouse urine that serves as an attractant to females is likely recognized by sensory neurons in the main olfactory epithelium [13]. In addition, innate behaviors such as mating and aggression, which are thought to be triggered by pheromonal cues, appear to require a functional olfactory epithelium [14,15]. Finally, suckling requires a functional main olfactory epithelium but not an intact vomeronasal organ in many animals, including rabbits and mice [16,17]. Taken together, these data suggest that the strict segregation of function originally posited for the main olfactory epithelium and the vomeronasal organ may not be entirely accurate [18]. An interesting question for the future is whether associative learning can be promoted by all pheromones or whether this property is the exclusive domain of pheromones recognized by the main olfactory epithelium.

The study by Coureaud *et al.* [4] immediately suggests interesting directions for future research. What is the neural locus for learning the paired odor? The main olfactory epithelium expresses a large family of genes encoding G-protein coupled olfactory receptors [19]. Which olfactory receptors recognize 2MB2, and is the entire complement of receptors for 2MB2 required for learning the paired odor? Do human infants learn to pair other cues with nursing? Olfaction is thought to play a minor role in initiating suckling in human infants (cf. rooting reflex) [1]. However, this does not preclude associative learning of previously irrelevant cues with nursing in humans. After all, Romulus, the mythical founder of Rome, was said to have been nursed by a wolf and fed by Picus, a woodpecker.

References

1. Blass, E.M., and Teicher, M.H. (1980). Suckling. Science *210*, 15–22.
2. Hudson, R. (1985). Do newborn rabbits learn the odor stimuli releasing nipple-search behavior? Dev. Psychobiol. *18*, 575–585.
3. Schaal, B., Coureaud, G., Langlois, D., Giniès, C., Sémon, E., and Perrier, G. (2003). Chemical and behavioral characterization of the rabbit mammary pheromone. Nature *424*, 68–72.
4. Coureaud, G., Moncomble, A.-S., Montigny, D., Dewas, M., Perrier, G., and Schaal, B. (2006). A pheromone that rapidly promotes learning in the newborn. Curr. Biol. *16*, 1956–1961.
5. Tinbergen, N. (1951). The study of instinct (New York: Oxford University Press.).
6. Halpern, M. (1987). The organization and function of the vomeronasal system. Annu. Rev. Neurosci. *10*, 325–362.
7. Wysocki, C.J. (1979). Neurobehavioral evidence for the involvement of the vomeronasal system in mammalian reproduction. Neurosci. Biobehav. Rev. *3*, 301–341.
8. Axel, R. (1995). The molecular logic of smell. Sci. Am. *273*, 154–159.
9. Dulac, C., and Torello, A.T. (2003). Molecular detection of pheromone signals in mammals: From genes to behavior. Nat. Rev. Neurosci. *4*, 551–562.
10. Keil, W., von Stralendorff, F., and Hudson, R. (1990). A behavioral bioassay for analysis of rabbit nipple-search pheromone. Physiol. Behav. *47*, 525–529.
11. Zarrow, M.X., Denenberg, V.H., and Anderson, C.O. (1965). Rabbit: Frequency of suckling in the pup. Science *150*, 1835–1836.
12. Raisman, G. (1972). An experimental study of the projection of the amygdala to the accessory olfactory bulb and its relationship to the concept of a dual olfactory system. Exp. Brain Res. *14*, 395–408.
13. Lin, D.Y., Zhang, S.Z., Block, E., and Katz, L.C. (2005). Encoding social signals in the mouse main olfactory bulb. Nature *434*, 470–477.
14. Mandiyan, V.S., Coats, J.K., and Shah, N.M. (2005). Deficits in sexual and aggressive behaviors in Cnga2 mutant mice. Nat. Neurosci. *8*, 1660–1662.
15. Yoon, H., Enquist, L.W., and Dulac, C. (2005). Olfactory inputs to hypothalamic neurons controlling reproduction and fertility. Cell *123*, 669–682.
16. Hudson, R., and Distel, H. (1986). Pheromonal release of suckling in rabbits does not depend on the vomeronasal organ. Physiol. Behav. *37*, 123–128.
17. Brunet, L.J., Gold, G.H., and Ngai, J. (1996). General anosmia caused by a targeted disruption of the mouse olfactory cyclic nucleotide-gated cation channel. Neuron *17*, 681–693.
18. Restrepo, D., Arellano, J., Oliva, A.M., Schaefer, M.L., and Lin, W. (2004). Emerging views on the distinct but related roles of the main and accessory olfactory systems in responsiveness to chemosensory signals in mice. Horm. Behav. *46*, 247–256.
19. Buck, L., and Axel, R. (1991). A novel multigene family may encode odorant receptors: a molecular basis for odor recognition. Cell *65*, 175–187.

Department of Anatomy, 1550 4th Street, MC 2722, University of California San Francisco, San Francisco, California 94158, USA.
E-mail: nms@ucsf.edu

DOI: 10.1016/j.cub.2006.09.001

Replicative Helicases: A Staircase with a Twist

The first crystal structure of a ring helicase encircling single-stranded DNA reveals a mechanism for ATP-dependent DNA translocation.

Mark S. Dillingham

Following their elucidation of the structure of DNA, Watson and Crick were quick to realise its important implications for DNA replication. As they appreciated, replication of helically intertwined DNA strands represents a major topological challenge [1]. One problem is that the information to be copied is locked within

anti-parallel phosphodiester chains. Before a replicative polymerase can access its template, the duplex must be separated into its component single-strands. This activity is catalysed by DNA helicases: enzymes that couple ATP hydrolysis to the unwinding of duplex nucleic acids. DNA helicases are ubiquitous, highly abundant, and function in many aspects of nucleic acid metabolism including replication, recombination, and repair. Although they come in many shapes and sizes, those helicases involved in genomic DNA replication are invariably hexameric rings that display structural homology to diverse groups of toroidal ATP-dependent motor proteins [2]. It is known that single-stranded DNA occupies the channel in the centre of the ring [3]. Therefore, these enzymes are thought to unwind duplex DNA by encircling and translocating along one strand while excluding the complementary strand to the outside of the ring. Until now, our understanding of the hexameric helicases has been limited by the lack of a structure with single-stranded DNA, and the molecular details of how ATP hydrolysis is coupled to unidirectional single-stranded DNA translocation have remained unclear.

This has now changed with the report by Enemark and Joshua-Tor [4] of the crystal structure of bovine papillomavirus E1 helicase in complex with single-stranded DNA, ADP and Mg^{2+}. E1 plays a central role in virus replication, being involved in both recognition of the origin of replication and DNA unwinding. As a member of helicase superfamily 3, E1 moves along single-stranded DNA in the 3′ to 5′ direction; it is also a member of the AAA+ class of ATPases [5]. In the structure (Figure 1), E1 lacking its amino-terminal origin-binding domain is assembled into the expected hexameric ring. Each subunit consists of a large AAA+ motor domain and a smaller oligomerization domain. The oligomerization domains form a stable collar that may function as a processivity factor. The AAA+ domains form a looser ring that deviates from exact six-fold symmetry. ADP molecules are located in nucleotide binding pockets at their interfaces, providing a basis for allosteric control of the AAA+ conformations around the ring in response to ATP binding and hydrolysis.

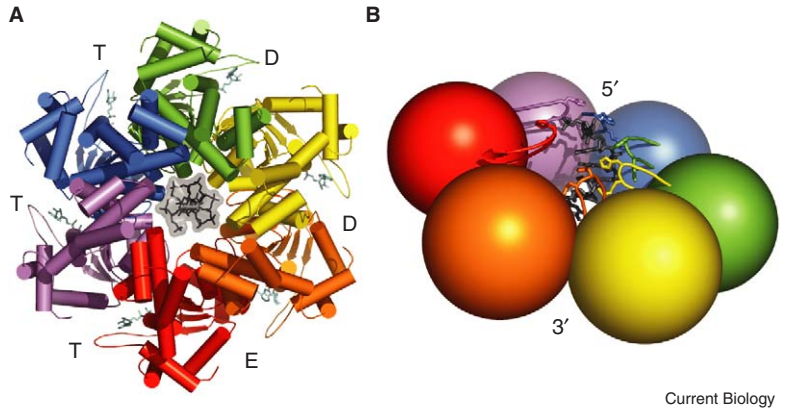

Figure 1. Structure of bovine papillomavirus E1 helicase in complex with single-stranded DNA, ADP and Mg^{2+}.

(A) The hexamer viewed from the front (5′ end of the single-stranded DNA). Each subunit of the hexamer is in a different color, ADP molecules are cyan, and single-stranded DNA is black. The status of each nucleotide binding pocket (T, D, or E) is indicated (see text). (B) A simplified view of the AAA+ domains bound to single-stranded DNA. The hairpins protrude into the central channel and contact single-stranded DNA via conserved lysine and histidine residues to form a 'spiral staircase' with the red hairpin in the highest position. (Figures were made using PYMOL http://pymol.sourceforge.net/).

Six bases of single-stranded DNA are bound snugly in the central channel by six protruding hairpin loops that progressively decrease in height around the ring. Consequently, the hairpin–DNA interactions resemble a spiral staircase that enforces radial asymmetry in the ring. Importantly, the height of each hairpin correlates with the status of the associated nucleotide binding pocket. Despite each of the six pockets being occupied by an ADP molecule, they are non-equivalent. The pockets associated with hairpins in the most elevated positions are designated 'ATP-type' (T) by virtue of the compact positioning of key catalytic residues around the bound nucleotide. The next pockets around the ring, designated 'ADP-type' (D), are less compact and associated with hairpins of intermediate height. The final pockets are associated with the lowest hairpins and are in the most open conformation representing an empty state (E).

From this key observation, Enemark and Joshua-Tor [4] propose a 'coordinated escort' mechanism for ATP-dependent unidirectional single-stranded DNA translocation (Figure 2). The transition of each nucleotide-binding pocket from T to D and then E state, mediated by ATP hydrolysis and release, drives the passage of each hairpin from the top to the bottom of the central channel, escorting its DNA cargo through the helicase. Upon release of single-stranded DNA at the bottom of the channel, the associated AAA+ domain binds ATP, returning its hairpin to the top of the staircase where it engages the next available DNA nucleotide and begins escorting it through the channel. The staircase of hairpin-single-stranded DNA contacts ensures coordinated movement of the six hairpins. Consequently, ATP binding, hydrolysis, and product release events take place in a sequential, rotary fashion around the ring and the enzyme smoothly ascends a spiral staircase of its own construction.

The proposed model implies a step size of one base per ATP, which is consistent with some kinetic measurements made in hexameric [6] and monomeric helicases [7]. This is thermodynamically inefficient,

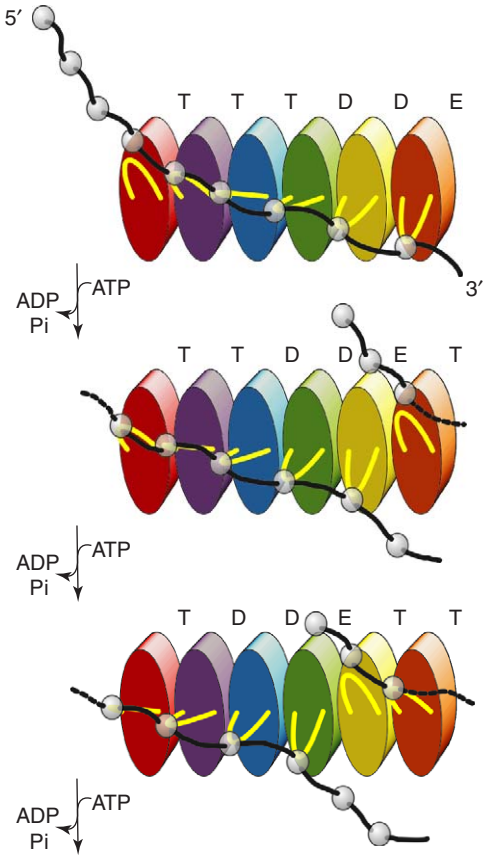

Figure 2. The coordinated escort mechanism for single-stranded DNA translocation.

Cartoon representation of the E1 hexamer opened into a line. Note that the red and orange subunits are in contact in the closed hexamer. The status of the nucleotide binding pockets is indicated (see text). Hairpins (yellow) each contact one DNA nucleotide (gray/black). The top panel is equivalent to the structure in Figure 1. Translocation of single-stranded DNA by one base step is driven by coordinated movement of all six hairpins in response to the net binding, hydrolysis and release of one ATP molecule (see text). Dotted lines in the single-stranded DNA indicate that it continues at the other side of the opened hexamer.

however, with some estimates suggesting that as many as 9–12 base pairs of duplex DNA could, theoretically, be separated by the turnover of a single ATP molecule [8]. Confirmation of the proposed mechanism will require direct measurement of a very small step size. In practice, this has proven to be a challenging task, but one that seems destined to yield to ever-improving single-molecule techniques [9]. Together with previous kinetic and crystallographic analysis of hexameric helicases [10–13], the E1 structure strongly suggests that ATP hydrolysis occurs sequentially at each subunit around the ring. However, it is not clear exactly when hydrolysis and product release occurs during the transit of each hairpin through the channel.

Alternative ATP hydrolysis mechanisms have been proposed for hexameric motors. For example, a structure of the closely related SV40 T antigen was used to support a concerted hydrolysis mechanism [14] and mutational analysis of the AAA+ motor ClpX supports a stochastic model [15]. Staircasing of DNA binding loops has also been observed in the superfamily 4 ring helicases that track in the opposite, 5′ to 3′, direction on single-stranded DNA [10]. In principle, they might operate by a mechanism akin to coordinated escort in reverse gear, or they may simply bind the single-stranded DNA in the opposite orientation. Other hexameric motors translocate double-stranded, rather than single-stranded DNA, while some work on completely unrelated polymer tracks such as peptide. It will be of particular interest to determine to what extent these diverse enzymes share a unifying underlying mechanism.

This appealing mechanism raises many questions. For example, it is not clear precisely how single-stranded DNA translocation leads to duplex DNA unwinding. Does the enzyme passively trap single-stranded DNA that becomes available through thermal fraying at the junction with double-stranded DNA, or does it generate force against the duplex that assists in its melting? Are there specific contacts with the duplex or the displaced (non-translocated) single-strand? Of course, replicative helicases do not act in isolation but as components of the replisome: a multi-component molecular machine. Structural studies of replicative helicases in complex with replication fork analogues and their protein partners will help us understand how they function in detail.

References

1. Watson, J.D., and Crick, F.H. (1953). Genetical implications of the structure of deoxyribonucleic acid. Nature *171*, 964–967.
2. Patel, S.S., and Picha, K.M. (2000). Structure and function of hexameric helicases. Annu. Rev. Biochem. *69*, 651–697.
3. Yu, X., Hingorani, M.M., Patel, S.S., and Egelman, E.H. (1996). DNA is bound within the central hole to one or two of the six subunits of the T7 DNA helicase. Nat. Struct. Biol. *3*, 740–743.
4. Enemark, E.J., and Joshua-Tor, L. (2006). Mechanism of DNA translocation in a replicative hexameric helicase. Nature *442*, 270–275.
5. Hickman, A.B., and Dyda, F. (2005). Binding and unwinding: SF3 viral helicases. Curr. Opin. Struct. Biol. *15*, 77–85.
6. Galletto, R., Jezewska, M.J., and Bujalowski, W. (2004). Unzipping mechanism of the double-stranded DNA unwinding by a hexameric helicase: quantitative analysis of the rate of the dsDNA unwinding, processivity and kinetic step-size of the Escherichia coli DnaB helicase using rapid quench-flow method. J. Mol. Biol. *343*, 83–99.
7. Dillingham, M.S., Wigley, D.B., and Webb, M.R. (2000). Demonstration of unidirectional single-stranded DNA translocation by PcrA helicase: measurement of step size and translocation speed. Biochemistry *39*, 205–212.
8. Lohman, T.M., and Bjornson, K.P. (1996). Mechanisms of helicase-catalyzed DNA unwinding. Annu. Rev. Biochem. *65*, 169–214.
9. Abbondanzieri, E.A., Greenleaf, W.J., Shaevitz, J.W., Landick, R., and Block, S.M. (2005). Direct observation of base-pair stepping by RNA polymerase. Nature *438*, 460–465.
10. Singleton, M.R., Sawaya, M.R., Ellenberger, T., and Wigley, D.B. (2000). Crystal structure of T7 gene 4 ring helicase indicates a mechanism for sequential hydrolysis of nucleotides. Cell *101*, 589–600.
11. Liao, J.C., Jeong, Y.J., Kim, D.E., Patel, S.S., and Oster, G. (2005). Mechanochemistry of t7 DNA helicase. J. Mol. Biol. *350*, 452–475.
12. Adelman, J.L., Jeong, Y.J., Liao, J.C., Patel, G., Kim, D.E., Oster, G., and Patel, S.S. (2006). Mechanochemistry of

transcription termination factor Rho. Mol. Cell *22*, 611–621.
13. Crampton, D.J., Mukherjee, S., and Richardson, C.C. (2006). DNA-induced switch from independent to sequential dTTP hydrolysis in the bacteriophage T7 DNA helicase. Mol. Cell *21*, 165–174.
14. Gai, D., Zhao, R., Li, D., Finkielstein, C.V., and Chen, X.S. (2004). Mechanisms of conformational change for a replicative hexameric helicase of SV40 large tumor antigen. Cell *119*, 47–60.
15. Martin, A., Baker, T.A., and Sauer, R.T. (2005). Rebuilt AAA + motors reveal operating principles for ATP-fuelled machines. Nature *437*, 1115–1120.

DNA: protein interactions unit, Department of Biochemistry, School of Medical Sciences, University of Bristol, University Walk, Bristol BS8 1TD, UK.
E-mail: Mark.Dillingham@bristol.ac.uk

DOI: 10.1016/j.cub.2006.08.074

Perception: Transient Disruptions to Neural Space–Time

How vision operates efficiently in the face of continuous shifts of gaze remains poorly understood. Recent studies show that saccades cause dramatic, but transient, changes in the spatial and also temporal tuning of cells in many visual areas, which may underly the perceptual compression of space and time, and serve to counteract the effects of the saccades and maintain visual stability.

David Burr[1] and Concetta Morrone[2]

It has long been known that saccades, the fast ballistic eye-movements that periodically reposition gaze on items of interest, present hefty challenges to the visual system. It somehow manages to annul these brisk movements from the retinal images in order to perceive a stable world [1]. Psychophysical studies show that spatial vision is grossly distorted at the time of saccades, resulting in a severe but transient compression of the spatial metric [2]: visual stimuli are seen to be much closer to each other than they actually are. Perhaps even more mysterious is the recent observation that time is also compressed around the time of saccades [3], so pairs of brief stimuli separated by 100 milliseconds are seen to be separated by only 50 milliseconds. The timecourse for temporal and spatial compression is very similar, suggesting that they are both manifestations of the same phenomena.

Ibbotson and colleagues [4,5] have recently reported that in cortical areas MT and MST of the macaque monkey, cells respond to visual motion generated by saccades sweeping over stationary texture with considerably shorter latency than they do to texture moving at comparable speeds during fixation: on average 30 milliseconds for saccade-elicited motion compared with 67 milliseconds during fixation (Figure 1). Interestingly, the shortening of latencies follows a different pattern in the two areas: in MST latencies halve during saccades, while in MT they seem to be all flattened to about 30 milliseconds, irrespective of the latency in normal viewing. In this issue of *Current Biology*, Ibbotson *et al.* [6] suggest that these changes in latency could underlie the psychophysically observed temporal compression. This idea is not unreasonable, as previous studies in macaque [7] have shown that areas MT and MST are strongly implicated in encoding of spatial position, and that their spatial code 'collapses' around the time of saccades, making these areas likely neural substrates for spatial compression.

It is clear that a reduction in latency could cause compression of time during some intervals. If the first stimulus were presented before the saccade, it would arrive in MT cells some 67 milliseconds later; but if the second bar, presented 100 ms after the first, were to occur near the saccade, it should have a shorter latency and arrive only 30 milliseconds later, 130 milliseconds after the presentation of the first bar: a difference of 63 rather than 100 milliseconds. The changes in latencies may also explain a particularly uncanny aspect of data our group has reported [3], the apparent inversion of temporal order at some specific conditions: if the second stimulus were subjected to shorter latencies than the first, it could well overtake it and be seen to arrive first. Indeed this would make good sense, as the psychophysically observed temporal inversion occurred only for stimuli presented within a very specific time window (60–80 milliseconds before saccadic onset), a tight range where it is feasible that the second but not the first may be subjected to peri-saccadic acceleration.

Ibbotson *et al.*'s [6] data are also consistent with another counterintuitive finding: that the precision for judging duration is better during saccades than during fixation. As Figure 1 shows, average response latencies of MT neurons are not only shorter during saccades than fixation, but the spread of latencies is considerably less, particularly for MT cells (reflected by the standard deviations, and by inspection of the scattergram). If these signals were used to judge duration, the decreased variability in the population should lead to the increased precision observed psychophysically.

Although the reduced latencies provide a good qualitative description for the effects of saccades on time perception, they fail quantitatively. While the temporal inversion occurred only at very specific times relative to saccade onset, strong (two-fold) compression of time occurred for a period of over 300 milliseconds, extending well before saccadic onset to well after its completion. As the stimulus pairs were separated by only